

BASIC CONCEPTS II

F. Caspers

CERN, Geneva, Switzerland

ABSTRACT

The concept of describing rf circuits in terms of waves is discussed and the relationships between commonly used matrices (S, T, ABCD, Y, Z, H, G) are defined. The signal flow graph (SFG) is introduced as a graphical means to visualize how waves propagate in an rf network. The properties of the most relevant passive rf devices (hybrids, couplers, non-reciprocal elements, etc.) are delineated and the corresponding Sparameters are given. For microwave integrated circuits (MIC's) planar transmission lines such as the microstrip line have become very important. A brief discussion on the Smith Chart concludes this paper.

1. INTRODUCTION

For the design of rf and microwave circuits a practical tool is required. The linear dimensions of the elements that are in use may be of the order of one wavelength or even larger. In this case the equivalent circuits which are commonly applied for lower frequencies lead to difficulties in the definition of voltages and currents. A description in terms of waves becomes more meaningful. These waves are scattered (reflected, transmitted) in rf networks. Having introduced certain definitions of the relation between voltages, currents and waves we discuss different matrices such as S-, T- and ABCD-matrix for the description of 2-port networks. Nowadays the calculation of complex microwave networks is usually carried out by means of computer codes. These apply matrix descriptions and conversions extensively. Another way to analyze microwave networks is by taking advantage of the signal flow graph (SFG). The SFG is a graphical representation of a system of linear equations and permits one to visualize how, for example, an incident wave propagates through the network. However, for a systematic analysis of large networks the SFG is not very convenient since the risk of overlooking a signal path increases rapidly with the size of the network. In a subsequent section the properties of typical microwave n-ports ($n = 1, 2, 3, 4$) are discussed. The n-ports include power dividers, directional couplers, circulators and 180° hybrids. Historically many microwave elements have been built first in waveguide technology. Today waveguide technology is rather restricted to high-power applications or for extremely high frequencies. Other less bulky types of transmission lines have been developed such as striplines and microstriplines. They permit the realisation of microwave integrated circuits (MIC's) or, if implemented on a semiconductor substrate, the monolithic microwave integrated circuits (MMIC's). This paper concludes with a description of the Smith Chart, a graphical method of evaluating the complex reflection coefficient for a given load. Several examples including the coupling of single-cell resonators are mentioned.

2. S-PARAMETERS

The abbreviation *S* has been derived from the word *scattering*. For high frequencies, it is convenient to describe a given network in terms of *waves* rather than voltages or currents. This permits an easier definition of reference planes. For practical reasons, the description in terms of in- and outgoing waves has been introduced. Now, a 4-pole network becomes a 2-port and a 2n-pole becomes an n-port. In the case of an odd pole number (e.g. 3-pole), a common reference point may be chosen, attributing one pole equally to two ports. Then a 3-pole is converted into a (3+1) pole or a 2-port. Rule: for an odd pole number add 1.

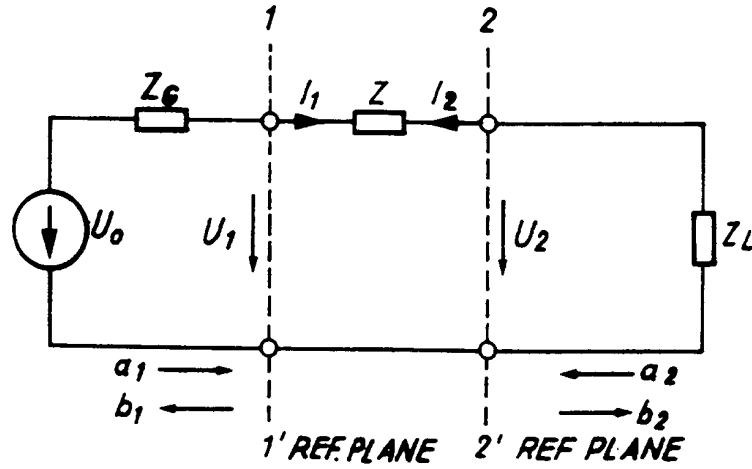


Fig. 1 2-port network

Let us start by considering a simple 2-port network. If $Z = 0$ and $Z_G = Z_L$ (Z_G and Z_L real) we have a matched load and $U_1 = U_2 = U_0/2$. The lines connecting the different elements (Z_G, Z, Z_L) in Fig. 1 are supposed to have no electrical length. Connections with an electrical length are drawn as double lines or as heavy lines. Now we would like to relate U_0, U_1, U_2 with a and b .

Definition:

All waves going towards the n-port are a (a_1, a_2, \dots, a_n). All waves travelling away from the n-port are b (b_1, b_2, \dots, b_n). The definition for the direction of the currents (generalization for an n-port) says that positive currents flow into the network according to Fig. 1. The wave a_1 is related to the maximum available power (matched load).

In order to give definitions that are consistent with the conservation of energy, the voltage is normalized to $\sqrt{Z_0}$. Z_0 is in general an arbitrary reference impedance, but is usually the characteristic impedance of a line (e.g. 50 Ω) and very often $Z_G = Z_0 = Z_L$.

$$\begin{aligned} a_1 &= \frac{U_0}{2\sqrt{Z_0}} = \frac{\text{incident voltage wave (port 1)}}{\sqrt{Z_0}} = \frac{U_1^i}{\sqrt{Z_0}} \\ b_1 &= \frac{U_1^r}{\sqrt{Z_0}} = \frac{\text{reflected voltage wave (port 1)}}{\sqrt{Z_0}} \end{aligned} \quad (1)$$

Note that a, b have the dimension $\sqrt{\text{power}}$ [1].

The power travelling towards port 1 is simply the available power from the source, i.e.

$$\begin{aligned} P_1^i &= \frac{1}{2} |a_1|^2 = \frac{|U_1^i|^2}{2Z_0} = \frac{|I_1^i|^2}{2} Z_0 \\ P_1^r &= \frac{1}{2} |b_1|^2 = \frac{|U_1^r|^2}{2Z_0} = \frac{|I_1^r|^2}{2} Z_0 \end{aligned} \quad (2)$$

In the case of a mismatched load Z_L there will be some power reflected towards the 2-port (from Z_L)

$$P_2^i = \frac{1}{2} |a_2|^2$$

There is also the outgoing wave of port 2 which may be considered as the superposition of a wave that has gone through the 2-port from the generator and a reflected part from the mismatched load. As we defined $a_1 = U_o/(2\sqrt{Z_o}) = U_i/\sqrt{Z_o}$, we can also quote $a_1 = I_i\sqrt{Z_o}$, and we obtain

$$\begin{aligned} a_i &= \frac{U_i + I_i Z_o}{2\sqrt{Z_o}} \\ b_i &= \frac{U_i - I_i Z_o}{2\sqrt{Z_o}} \end{aligned} \quad i = 1, 2 \quad (3.1)$$

$$\begin{aligned} U_i &= \sqrt{Z_o}(a_i + b_i) = U_i^i + U_i^r \\ I_i &= \frac{1}{\sqrt{Z_o}}(a_i - b_i) = \frac{U_i^i - U_i^r}{Z_o} \end{aligned} \quad (3.2)$$

$$\begin{aligned} P_i &= \frac{1}{2} \text{Re}\{U_i I_i^*\} \\ P_i &= \frac{1}{2} \text{Re}\{(a_i a_i^* - b_i b_i^*) + (a_i^* b_i - a_i b_i^*)\} \\ P_i &= \frac{1}{2} (a_i a_i^* - b_i b_i^*) \end{aligned} \quad (3.3)$$

with $u(t) = \text{Re}\{Ue^{j\omega t}\}$.

The relation between a_i and b_i ($i = 1 \dots n$) can be written as a system of n linear equations (a_i being the independent variable, b_i the dependent variable)

$$\begin{aligned} b_1 &= S_{11}a_1 + S_{12}a_2 \\ b_2 &= S_{21}a_1 + S_{22}a_2 \end{aligned} \quad \text{or} \quad (B) = (S)(A). \quad (4)$$

The physical meaning of S_{11} is the input reflection coefficient with the output of the network terminated by a matched load ($a_2 = 0$). S_{21} is the forward transmission (from port 1 to port 2), S_{12} the reverse transmission and S_{22} the output reflection coefficient.

Important note: when measuring the S-parameters of an n -port, all n ports must be terminated by a matched load (not necessarily equal for all ports), including the port connected to the generator (matched generator).

Using Eq. (3.1) we find ($Z = 0$)

$$S_{11} = \left. \frac{b_1}{a_1} \right|_{a_2=0} = \frac{U_1 - I_1 Z_0}{U_1 + I_1 Z_0} = \frac{Z_L - Z_0}{Z_L + Z_0} = \rho = \frac{(Z_L/Z_0) - 1}{(Z_L/Z_0) + 1} \quad (5.1)$$

which is the familiar formula for the reflection coefficient ρ (often also denoted Γ).

For the example in Fig. 1, with $Z_G = Z_L = Z_0$, we obtain:

$$\begin{aligned} U_2 &= U_0 \frac{Z_L}{2Z_L + Z} = \frac{U_0}{2} S_{21}, \quad S_{21} = \frac{2Z_L}{2Z_L + Z} \\ U_1 &= U_0 \frac{Z_L + Z}{2Z_L + Z} = \frac{U_0}{2} (1 + S_{11}), \quad S_{11} = \frac{Z}{2Z_L + Z} \end{aligned} \quad (5.2)$$

The scattering matrix (S-matrix) introduced in Eq. (4) is a very convenient way to describe an n-port in terms of waves. The S-matrix is, in particular, very well adapted to measurements. However, in order to characterize the response of a number of cascaded 2-ports, it is desirable to use a different description since the S-matrix of several cascaded 2-ports is not easy to work out in a straightforward manner. We use the so-called T-matrix [2]

$$\begin{pmatrix} b_1 \\ a_1 \end{pmatrix} = \begin{pmatrix} T_{11} & T_{12} \\ T_{21} & T_{22} \end{pmatrix} \begin{pmatrix} a_2 \\ b_2 \end{pmatrix} \quad (6)$$

As the transmission matrix (T-matrix) simply links the in- and outgoing waves in a way different from the S-matrix, one may convert the matrix elements mutually

$$\begin{aligned} T_{11} &= S_{12} - \frac{S_{22}S_{11}}{S_{21}}, \quad T_{12} = \frac{S_{11}}{S_{21}} \\ T_{21} &= -\frac{S_{22}}{S_{21}}, \quad T_{22} = \frac{1}{S_{21}} \end{aligned} \quad (7)$$

Caution: the T-parameters are indeterminate for $S_{21} = 0$.

The physical meaning of the individual elements of a T-matrix is not as evident as for the S-matrix, and the T-matrix is rather a mathematical tool for the calculation of cascaded 2-ports. The T-matrix T_M of m cascaded 2-ports yields (as in [2, 3]):

$$(T_M) = (T_1) \cdot (T_2) \cdots (T_m) \quad (8.1)$$

Note that in the literature [2-10] different definitions of the T-matrix can be found and the individual matrix elements depend on the definition used.

In Eqs. (6) and (7), the independent variables are the output waves (port 2) and from this the waves at the input of the 2-port are worked out. This implies, for the cascade, a matrix multiplication from "left" to "right", cf. Eq. (8.1). The other definition takes a_1 and b_1 as independent variables.

$$\begin{pmatrix} b_2 \\ a_2 \end{pmatrix} = \begin{pmatrix} \tilde{T}_{11} & \tilde{T}_{12} \\ \tilde{T}_{21} & \tilde{T}_{22} \end{pmatrix} \begin{pmatrix} a_1 \\ b_1 \end{pmatrix} \quad (8.2)$$

and for this case

$$\begin{aligned}\tilde{T}_{11} &= S_{21} - \frac{S_{22}S_{11}}{S_{12}}, & \tilde{T}_{12} &= \frac{S_{22}}{S_{12}} \\ \tilde{T}_{21} &= -\frac{S_{11}}{S_{12}}, & \tilde{T}_{22} &= \frac{1}{S_{12}}.\end{aligned}\tag{8.3}$$

Then, for the cascade, we obtain

$$\tilde{T}_M = \tilde{T}_m \tilde{T}_{m-1} \cdots (\tilde{T}_2)(\tilde{T}_1)\tag{8.4}$$

i.e. a matrix multiplication from "right" to "left".

In the following, the definition using Eq. (6) will be applied.

In practice, after having carried out the T-matrix multiplication, one would like to return to S-parameters

$$\begin{aligned}S_{11} &= \frac{T_{12}}{T_{22}}, & S_{12} &= T_{11} - \frac{T_{12}T_{21}}{T_{22}} \\ S_{21} &= \frac{1}{T_{22}}, & S_{22} &= -\frac{T_{21}}{T_{22}}.\end{aligned}\tag{9}$$

For a reciprocal network ($S_{21} = S_{12}$ or more generally $S_{ij} = S_{ji}$) the T-parameters have to meet the condition ($\det T = 1$)

$$T_{11}T_{22} - T_{12}T_{21} = 1.\tag{10}$$

So far, we have been discussing the properties of the 2-port mainly in terms of incident (a) and reflected (b) waves. Returning to Fig. 1 and Eqs. (1) to (3) the description in voltages and currents is briefly carried out. Considering the current I_1 and I_2 as independent variables, the dependent variables U_1 and U_2 are written as a Z-matrix:

$$\begin{aligned}U_1 &= Z_{11}I_1 + Z_{12}I_2 \\ U_2 &= Z_{21}I_1 + Z_{22}I_2\end{aligned}\quad \text{or} \quad (U) = (Z) \cdot (I)\tag{11}$$

where Z_{11} and Z_{22} are the input and output impedance, respectively. When measuring Z_{11} , the output of the 2-port (or, in general, all other ports) has to be open (no matched load as for the S-parameter measurement).

In an analogous manner, a Y-matrix (admittance matrix) can be defined as

$$\begin{aligned}I_1 &= Y_{11}U_1 + Y_{12}U_2 \\ I_2 &= Y_{21}U_1 + Y_{22}U_2\end{aligned}\quad \text{or} \quad (I) = (Y) \cdot (U) \quad .\tag{12}$$

Similarly to the S-matrix, the Z- and Y-matrices are not easy to apply for cascaded 4-poles (2-ports). Thus, the so-called ABCD-matrix (or A-matrix) has been introduced as a suitable cascaded network description in terms of voltages and currents (Fig. 1)

$$\begin{pmatrix} U_1 \\ I_1 \end{pmatrix} = \begin{pmatrix} A & B \\ C & D \end{pmatrix} \begin{pmatrix} U_2 \\ -I_2 \end{pmatrix} = \begin{pmatrix} A_{11} & A_{12} \\ A_{21} & A_{22} \end{pmatrix} \begin{pmatrix} U_2 \\ -I_2 \end{pmatrix}. \quad (13)$$

With the direction of I_2 chosen in Fig. 1 a minus sign appears for I_2 since $-I_2$ of a first 4-pole becomes I_1 in the next one.

It can be shown that the ABCD-matrix of two or more cascaded 4-poles becomes the matrix product of the individual ABCD-matrices [3]

$$\begin{pmatrix} A & B \\ C & D \end{pmatrix}_k = \begin{pmatrix} A & B \\ C & D \end{pmatrix}_1 \begin{pmatrix} A & B \\ C & D \end{pmatrix}_2 \cdots \begin{pmatrix} A & B \\ C & D \end{pmatrix}_k. \quad (14)$$

In practice, the *normalized* ABCD-matrix is usually applied. It has dimensionless elements only and is obtained by dividing B by Z_0 the reference impedance, and multiplying C with Z_0 . For example, the impedance Z (Fig. 1) with $Z_G = Z_L = Z_0$ would have the normalized ABCD-matrix [3, 4]

$$\begin{pmatrix} A & B \\ C & D \end{pmatrix}_N = \begin{pmatrix} 1 & Z/Z_0 \\ 0 & 1 \end{pmatrix}.$$

The elements of the S-matrix are related as

$$\begin{aligned} S_{11} &= \frac{A+B-C-D}{A+B+C+D}, & S_{12} &= \frac{2 \det A}{A+B+C+D} \\ S_{21} &= \frac{2}{A+B+C+D}, & S_{22} &= \frac{-A+B-C+D}{A+B+C+D} \end{aligned} \quad (15)$$

to the elements normalized of the ABCD-matrix. Furthermore, the H-matrix (hybrid) and G (inverse hybrid) will be mentioned as they are very useful for certain 2-port interconnections [3].

$$\begin{aligned} U_1 &= H_{11}I_1 + H_{12}U_2 \\ I_2 &= H_{21}I_1 + H_{22}U_2 \end{aligned} \quad \text{or} \quad \begin{pmatrix} U_1 \\ I_2 \end{pmatrix} = (H) \cdot \begin{pmatrix} I_1 \\ U_2 \end{pmatrix} \quad (16)$$

and

$$\begin{aligned} I_1 &= G_{11}U_1 + G_{12}I_2 \\ U_1 &= G_{12}U_1 + G_{22}I_2 \end{aligned} \quad \text{or} \quad \begin{pmatrix} I_1 \\ U_2 \end{pmatrix} = (G) \cdot \begin{pmatrix} U_1 \\ I_2 \end{pmatrix}. \quad (17)$$

All these different matrix forms may appear rather confusing, but they are applied in particular, in computer codes for rf and microwave network evaluation. As an example, in Fig. 2, the four basic possibilities of interconnecting 2-ports (besides the cascade) are shown. In simple cases, one may work with S-matrices directly, eliminating the unknown waves at the connecting points by rearranging the S-parameter equations.

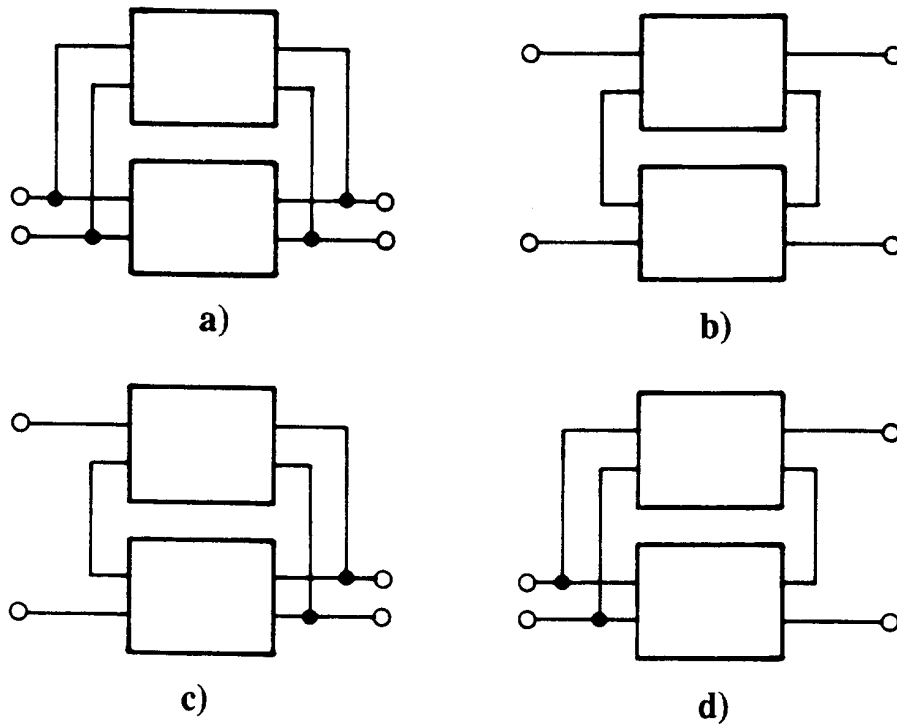


Fig. 2 Basic interconnections of 2-ports [1].
a) Parallel-parallel connection; add Y-matrix
b) Series-series connection; add Z-matrix
c) Series-parallel connection; add H-matrix
d) Parallel-series connection; add G-matrix [3].

Figures 3 show ABCD-, S- and T-matrices (reproduced with the permission of the publishers [3]).

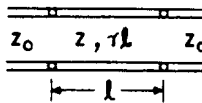
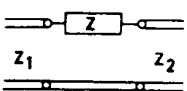
Element	ABCD-matrix	S-matrix	T-matrix
1. A transmission line section 	$\begin{bmatrix} \text{Ch} & Z \text{ Sh} \\ \frac{\text{Sh}}{Z} & \text{Ch} \end{bmatrix}$	$\frac{1}{D_s} \begin{bmatrix} (Z^2 - Z_o^2) \text{Sh} & 2ZZ_o \\ 2ZZ_o & (Z^2 - Z_o^2) \text{Sh} \end{bmatrix}$	$\begin{bmatrix} \text{Ch} - \frac{Z^2 + Z_o^2}{2ZZ_o} \text{Sh} & \frac{Z^2 - Z_o^2}{2ZZ_o} \text{Sh} \\ -\frac{Z^2 - Z_o^2}{2ZZ_o} \text{Sh} & \text{Ch} + \frac{Z^2 + Z_o^2}{2ZZ_o} \text{Sh} \end{bmatrix}$
where $\text{Sh} = \sinh \gamma l$, $\text{Ch} = \cosh \gamma l$ and $D_s = 2ZZ_o \text{Ch} + (Z^2 + Z_o^2) \text{Sh}$			
2. A series impedance 	$\begin{bmatrix} 1 & Z \\ 0 & 1 \end{bmatrix}$	$\frac{1}{D_s} \begin{bmatrix} Z + Z_2 - Z_1 & 2\sqrt{Z_1 Z_2} \\ 2\sqrt{Z_1 Z_2} & Z + Z_1 - Z_2 \end{bmatrix}$	$\frac{1}{D_t} \begin{bmatrix} Z_1 + Z_2 - Z & Z_2 - Z_1 + Z \\ Z_2 - Z_1 - Z & Z_1 + Z_2 - Z \end{bmatrix}$
where $D_s = Z + Z_1 + Z_2$ and $D_t = 2\sqrt{Z_1 Z_2}$			

Fig. 3 ABCD-, S- and T-matrices for the elements shown.

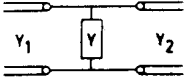
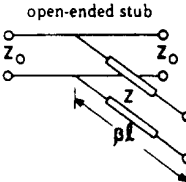
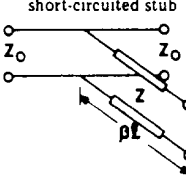
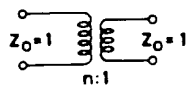
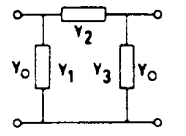
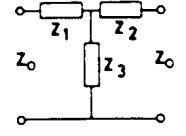
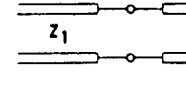
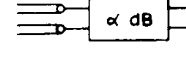
Element	ABCD-matrix	S-matrix	T-matrix
3. A shunt admittance 	$\begin{bmatrix} 1 & 0 \\ Y & 1 \end{bmatrix}$	$\frac{1}{D_s} \begin{bmatrix} Y_1 - Y_2 - Y & \sqrt{2Y_1Y_2} \\ 2\sqrt{Y_1Y_2} & Y_2 - Y_1 - Y \end{bmatrix}$	$\frac{1}{D_t} \begin{bmatrix} Y_1 + Y_2 - Y & Y_1 - Y_2 - Y \\ Y_1 - Y_2 + Y & Y_1 + Y_2 + Y \end{bmatrix}$
	where $D_s = Y + Y_1 + Y_2$ and $D_t = 2\sqrt{Y_1Y_2}$		
4. A shunt-connected open-ended stub 	$\begin{bmatrix} 1 & 0 \\ \frac{1}{jZT} & 1 \end{bmatrix}$	$\frac{1}{D_s} \begin{bmatrix} -1 & D_s - 1 \\ D_s - 1 & -1 \end{bmatrix}$	$\begin{bmatrix} 1 - \frac{Z_0}{2Z} T & -j \frac{Z_0}{2Z} T \\ j \frac{Z_0}{2Z} T & 1 + j \frac{Z_0}{2Z} T \end{bmatrix}$
	where $T = \tan \beta l$ and $D_s = 1 + 2jZT / Z_0$		
5. A shunt-connected short-circuited stub 	$\begin{bmatrix} 1 & 0 \\ jT/Z & 1 \end{bmatrix}$	$\frac{1}{D_s} \begin{bmatrix} 1 & D_s + 1 \\ D_s + 1 & 1 \end{bmatrix}$	$\begin{bmatrix} 1 + j \frac{Z_0}{2ZT} & j \frac{Z_0}{2ZT} \\ -j \frac{Z_0}{2ZT} & 1 - j \frac{Z_0}{2ZT} \end{bmatrix}$
	where $T = \tan \beta l$ and $D_s = -1 + 2jZ / (Z_0 T)$		
6. An ideal transformer 	$\begin{bmatrix} n & 0 \\ 0 & 1/n \end{bmatrix}$	$\frac{1}{n^2 + 1} \begin{bmatrix} n^2 - 1 & 2n \\ 2n & 1 - n^2 \end{bmatrix}$	$\frac{1}{2n} \begin{bmatrix} n^2 + 1 & n^2 - 1 \\ n^2 - 1 & n^2 + 1 \end{bmatrix}$
7. π -network 	$\begin{bmatrix} 1 + \frac{Y_2}{Y_3} & \frac{1}{Y_3} \\ \frac{D}{Y_3} & 1 + \frac{Y_1}{Y_3} \end{bmatrix}$	$\frac{1}{D_s} \begin{bmatrix} Y_0^2 - PY_0 - D & 2Y_0Y_3 \\ 2Y_0Y_3 & Y_0^2 + PY_0 - D \end{bmatrix}$	$\frac{1}{2Y_0Y_3} \begin{bmatrix} -Y_0^2 + QY_0 - D & Y_0^2 - PY_0 - D \\ -Y_0^2 - PY_0 + D & Y_0^2 + QY_0 + D \end{bmatrix}$
	where $D_s = Y_0^2 + QY_0 + D$, $D = Y_1Y_2 + Y_2Y_3 + Y_3Y_1$, $Q = Y_1 + Y_2 + 2Y_3$ and $P = Y_1 - Y_2$		
8. T-network 	$\begin{bmatrix} 1 + \frac{Z_1}{Z_3} & \frac{D}{Z_3} \\ \frac{1}{Z_3} & 1 + \frac{Z_2}{Z_3} \end{bmatrix}$	$\frac{1}{D_s} \begin{bmatrix} -Z_0^2 + PZ_0 + D & 2Z_0Z_3 \\ 2Z_0Z_3 & -Z_0^2 - PZ_0 + D \end{bmatrix}$	$\frac{1}{2Z_0Z_3} \begin{bmatrix} -Z_0^2 + QZ_0 - D & -Z_0^2 + PZ_0 + D \\ Z_0^2 + PZ_0 - D & Z_0^2 + QZ_0 + D \end{bmatrix}$
	where $D_s = Z_0^2 + QZ_0 + D$, $D = Z_1Z_2 + Z_2Z_3 + Z_3Z_1$, $Q = Z_1 + Z_2 + 2Z_3$ and $P = Z_1 - Z_2$		
9. A transmission line junction 	$\begin{bmatrix} 1 & 0 \\ 0 & 1 \end{bmatrix}$	$\frac{1}{D_s} \begin{bmatrix} Z_2 - Z_1 & 2\sqrt{Z_1Z_2} \\ 2\sqrt{Z_1Z_2} & Z_1 - Z_2 \end{bmatrix}$	$\frac{1}{D_t} \begin{bmatrix} Z_1 + Z_2 & Z_2 - Z_1 \\ Z_2 - Z_1 & Z_1 + Z_2 \end{bmatrix}$
	where $D_s = Z_1 + Z_2$ and $D_t = 2\sqrt{Z_1Z_2}$		
10. An α -dB attenuator 	$\begin{bmatrix} \frac{A+B}{2} & Z_0 \left(\frac{A-B}{2} \right) \\ \frac{A-B}{2Z_0} & \frac{A+B}{2} \end{bmatrix}$	$\begin{bmatrix} 0 & B \\ B & 0 \end{bmatrix}$	$\begin{bmatrix} -A & 0 \\ 0 & A \end{bmatrix}$
	where $A = 10^{\alpha/20}$ and $B = 1/A$		

Fig. 3 (continued) ABCD-, S- and T-matrices for the elements shown.

3. SIGNAL FLOW GRAPH (SFG)

The SFG is a graphical representation of a system of linear equations having the general form:

$$(Y) = (M)(X) + (M')(Y) \quad (18)$$

where (M) and (M') are square matrices with n rows and columns, (X) represents the n independent variables (sources) and (Y) the n dependent variables. The elements of (M) and (M') appear as transmission coefficients of the signal path. For practical work with S-parameter Eq. (18) sometimes (no signal loops) reduces to

$$(Y) = (M)(X) \quad \text{or} \quad (B) = (S)(A) . \quad (19)$$

The purpose of the SFG is to visualize physical relations and to provide a solution algorithm of Eq. (18) by applying a few rather simple rules:

1. The SFG has a number of points (nodes) each representing a single wave a_i or b_i .
2. Nodes are connected by branches (arrows), each representing one S-parameter and indicating direction.
3. A node may be the beginning or the end of a branch (arrow).
4. Nodes showing no branches pointing towards them are *source nodes*. All other nodes are *dependent signal nodes*.
5. Each node signal represents the sum of the signals carried by all branches entering it.
6. The transmission coefficients of parallel signal paths are to be added.
7. The transmission coefficients of cascaded signal paths are to be multiplied.
8. An SFG is feedback-loop free if a numbering of all nodes can be found such that every branch points from a node of lower number towards one of higher number.
9. A first-order loop is the product of branch transmissions, starting from a node and going along the arrows back to that node without touching the same node more than once. A second-order loop is the product of two non-touching first-order loops, and an n^{th} -order loop is the product of any n non-touching first-order loops.
10. An elementary loop with the transmission coefficient S beginning and ending at a node N may be replaced by a branch $(1-S)^{-1}$ between two nodes N_1 and N_2 , going from N_1 to N_2 . N_1 has all signals (branches) previously entering N , and N_2 is linked to all signals previously leaving from N .

In order to determine the ratio T of a dependent to an independent variable the so-called "non-touching loop rule", also known as Mason's rule, may be applied [11]

$$T = \frac{P_1[1 - \Sigma L(1)^{(1)} + \Sigma L(2)^{(1)} - \dots] + P_2[1 - \Sigma L(1)^{(2)} \dots]}{1 - \Sigma L(1) + \Sigma L(2) - \Sigma L(3) + \dots} \quad (20)$$

where:

- P_n are the different signal paths between the source and the dependent variable.
- $\Sigma L(1)^{(1)}$ represents the sum of all first-order loops not touching path 1, and $\Sigma L(2)^{(1)}$ is the sum of all second-order loop not touching path 1.

Analogously $\Sigma L(1)^{(2)}$ is the sum of all first-order loops in path 2.

- The expressions $\Sigma L(1)$, $\Sigma L(2)$ etc. in the denominator are the sums of all first-, second-, etc. order loops in the network considered.

As all this may sound complicated, let us look at a few examples.

Examples

We are looking for the input reflection coefficient of a 2-port with a non-matched load ρ_L and a matched generator (source) ($\rho_S = 0$) to start with. ρ_L , ρ_S are often written as Γ_L , Γ_S .

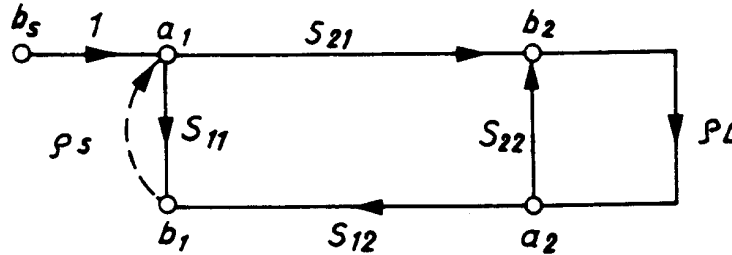


Fig. 4 2-port with non-matched load

By reading directly from the SFG (Fig. 4) we obtain

$$\frac{b_1}{a_1} = S_{11} + S_{21} \frac{\rho_L}{1 - S_{22}\rho_L} S_{12} \quad (21)$$

or by formally applying Eq. (20) (Mason's rule)

$$\frac{b_1}{a_1} = \frac{S_{11}(1 - S_{22}\rho_L) + S_{21}\rho_L S_{12}}{1 - S_{22}\rho_L} \quad (22)$$

As a more complicated example one may add a mismatch to the source (ρ_S = dashed line in Fig. 4) and ask for b_1/b_S

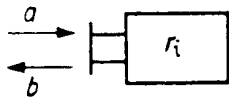
$$\frac{b_1}{b_S} = \frac{S_{11}(1 - S_{22}\rho_S) + S_{21}\rho_S S_{12}}{1 - (S_{11}\rho_S + S_{22}\rho_L + S_{12}\rho_L S_{21}\rho_S) + S_{11}\rho_S S_{22}\rho_L} \quad (23)$$

As we have seen in this rather easy configuration, the SFG is a convenient tool for the analysis of *simple* circuits [8, 12]. For more complex networks there is a considerable risk that a signal path may be overlooked and the analysis soon becomes complicated. When applied to S-matrices, the solution may sometimes be read directly from the diagram. The SFG is also a useful way to gain insight into other networks, such as feedback systems. But with the availability of powerful computer codes, the need to use the SFG has to some extent been reduced.

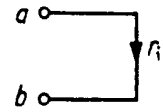
Element

S-matrix

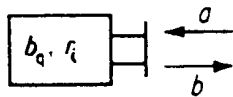
SFG



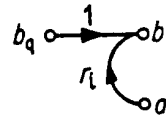
$$b = r_1 a$$



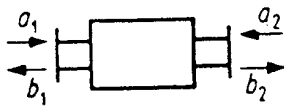
a) Passive one-port



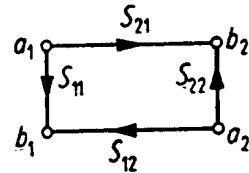
$$b = b_q + r_1 a$$



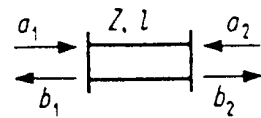
b) Active one-port



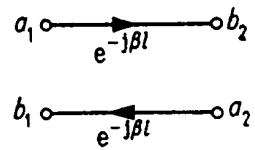
$$\mathbf{S} = \begin{pmatrix} S_{11} & S_{12} \\ S_{21} & S_{22} \end{pmatrix}$$



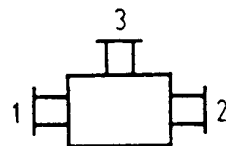
c) Passive two-port



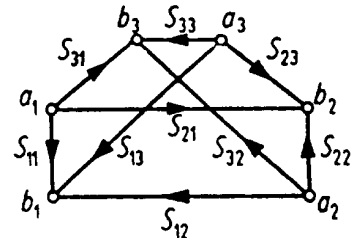
$$\mathbf{S} = \begin{pmatrix} 0 & e^{-j\beta l} \\ e^{-j\beta l} & 0 \end{pmatrix}$$



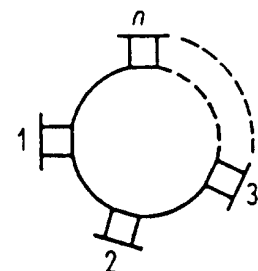
d) Lossless line (length ℓ) matched



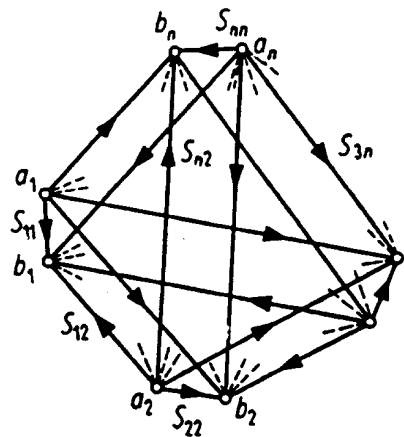
$$\mathbf{S} = \begin{pmatrix} S_{11} & S_{12} & S_{13} \\ S_{21} & S_{22} & S_{23} \\ S_{31} & S_{32} & S_{33} \end{pmatrix}$$



e) Passive 3-port



$$\mathbf{S} = \begin{pmatrix} S_{11} & S_{12} & \dots & S_{1n} \\ S_{21} & S_{22} & \dots & S_{2n} \\ \dots & \dots & \dots & \dots \\ S_{n1} & S_{n2} & \dots & S_{nn} \end{pmatrix}$$



f) Passive n-port

Fig. 5 SFG of different multiports (reproduced with the permission of the author [12])

- As a further example to exercise the methods mentioned so far
- elimination of waves at connecting points,
 - T-matrices,
 - SFG,

the following problem is suggested:

Cascade of two 2-ports (S_A), (S_B). Work out S_{11AB} , S_{12AB} , S_{21AB} and S_{22AB} .

4 PROPERTIES OF THE S-MATRIX OF AN N-PORT

A generalized n-port has n^2 scattering coefficients. All S_{ij} may be independent and different. In practice, due to symmetry, reciprocity, etc. the number of independent S_{ij} may be much smaller. In the case of transmission symmetry ($S_{ij} = S_{ji}$) the n-port is reciprocal. Reciprocal n-ports are structures made from resistors, inductors, capacitors and transformers. Examples for non-reciprocal networks are: amplifiers, structures with biased ferrites and charged particle currents (travelling wave tube, beam transfer function (BTF) between pickup and kicker; $S_{ij} \neq S_{ji}$). The elements on the main diagonal of the S-matrix (S_{ij} , $i = 1 \dots n$) are the input reflection coefficients (all other ports terminated by a matched load).

A passive n-port (for any external load) does not emit, on average, more power than it absorbs. For the lossless case the S-matrix becomes unitary, i.e.

$$(S^*)^T(S) = (1) \quad \text{or} \quad (S^*)^T = (S)^{-1} \quad (24.1)$$

This means for $n = 2$

$$(S^*)^T(S) = \begin{pmatrix} S_{11}^* & S_{21}^* \\ S_{12}^* & S_{22}^* \end{pmatrix} \begin{pmatrix} S_{11} & S_{12} \\ S_{21} & S_{22} \end{pmatrix} = \begin{pmatrix} 1 & 0 \\ 0 & 1 \end{pmatrix}$$

$$|S_{11}|^2 + |S_{21}|^2 = 1 \quad (24.2)$$

$$|S_{12}|^2 + |S_{22}|^2 = 1 \quad (24.3)$$

$$S_{11}^* S_{12} + S_{21}^* S_{22} = 0 \quad (24.4)$$

With $|S_{11}| \cdot |S_{12}| = |S_{21}| \cdot |S_{22}|$ from Eq. (24.3) and

$$-\text{arc}S_{11} + \text{arc}S_{12} = -\text{arc}S_{21} + \text{arc}S_{22} \pm \pi \quad (24.5)$$

we obtain

$$|S_{11}| = |S_{22}|, \quad |S_{12}| = |S_{21}|$$

$$|S_{11}| = \sqrt{1 - |S_{12}|^2} \quad (25)$$

Any lossless 2-port can be characterized by one modulus and three angles.

S-parameters are complex and frequency dependent. They change their phase when the reference plane is moved. Often the S-parameters can be determined only from geometrical symmetry and, if the circuit is lossless, using the relation $(S^*)^T \cdot (S) = 1$.

Examples of S-matrices of 1- and 2-ports:

1-port

Ideal short	$S_{11} = -1$
General short	$S_{11} = -1 e^{-2\gamma\ell}$
Ideal termination	$S_{11} = 0$
General load	$0 \leq S_{11} \leq 1$
	$0 \leq \arg S_{11} \leq \pi$
Active termination (reflection amplifier)	$ S_{11} > 1$

2-port

- a) Homogeneous line (length ℓ)
- $$\begin{aligned} S_{11} &= S_{22} = 0 \\ S_{12} &= S_{21} = e^{-\gamma\ell} \\ \text{Lossless case} \quad |S_{21}| &= |S_{12}| = 1 \end{aligned}$$
- b) Ideal phase shifter
- $$\begin{aligned} S_{11} &= S_{22} = 0 \\ S_{12} &= e^{-j\phi_{12}} \end{aligned}$$
- Reciprocal phase shifter $\phi_{12} = \phi_{21}$
- Non-reciprocal phase shifter (gyrator) $\phi_{12} - \phi_{21} = \pi$
- NB: $(S^*)^T(S) = 1$ does not apply because Eq. (24.5) is not met for the gyrator, which is lossless but non-reciprocal.
- c) Ideal, reciprocal attenuator
- $$\begin{aligned} S_{11} &= S_{22} = 0 \\ S_{12} &= S_{21} = |S_{12}| e^{-j\phi} \\ 0 &\leq |S_{21}| \leq 1 \\ \alpha [\text{dB}] &= 10 \log(1/|S_{21}|^2) = -20 \log |S_{21}| \end{aligned}$$
- Example: $\alpha_{21} = 40 \text{ dB} \rightarrow |S_{21}| = 0.01$
- d) Non-reciprocal attenuator, ideal isolator
- $$\begin{aligned} S_{11} &= S_{22} = 0 \\ |S_{21}| &= 1 \\ |S_{12}| &= 0 \end{aligned}$$
- The isolator has losses!
- e) Ideal amplifier
- $$\begin{aligned} S_{11} &= S_{22} = 0 \\ |S_{21}| &> 1 \\ |S_{12}| &= 0 \end{aligned}$$

3-port

Several types of 3-ports are in use: e.g. power divider, circulator, E- and H-plane, "T"-junctions. Applying the condition $(S^*)^T(S) = (1)$ leads to a set of equations

$$\begin{aligned} |S_{11}|^2 + |S_{21}|^2 + |S_{31}|^2 &= 1, & S_{11}^* S_{12} + S_{21}^* S_{22} + S_{31}^* S_{32} &= 0 \\ |S_{12}|^2 + |S_{22}|^2 + |S_{32}|^2 &= 1, & S_{11}^* S_{13} + S_{21}^* S_{23} + S_{31}^* S_{33} &= 0 \\ |S_{13}|^2 + |S_{23}|^2 + |S_{33}|^2 &= 1, & S_{12}^* S_{13} + S_{22}^* S_{23} + S_{32}^* S_{33} &= 0 \end{aligned} \quad (26)$$

and it can be shown that there is no lossless, reciprocal 3-port matched at all ports. The resistive power divider: matched at all ports, reciprocal, lossy. The 3-port circulator is lossless, matched at all ports, non-reciprocal. In other words: a reciprocal, lossless 3-port cannot be matched at all ports, or a lossless 3-port matched at all ports cannot be reciprocal.

Let us look at a few examples.

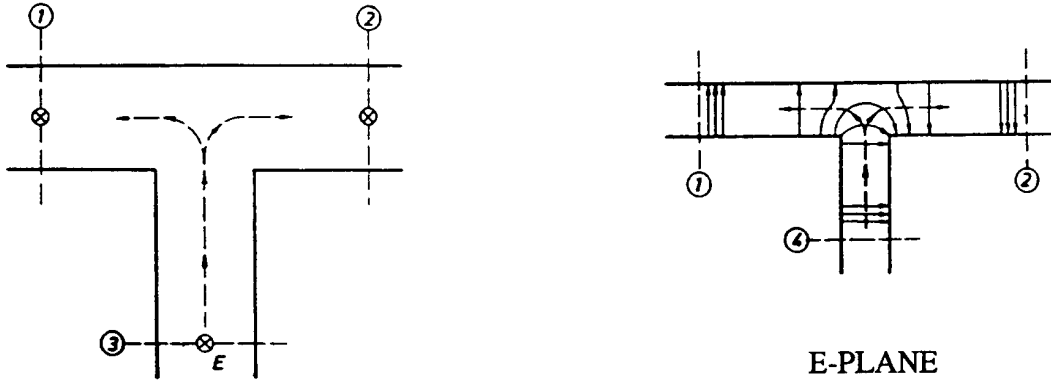


Fig. 6 H_{10} waveguide "T"s; H-plane, E-plane.

Applying Eq. (26) in Fig. 6, symmetry considerations and appropriate reference planes, one finds

$$S_H = \frac{1}{2} \begin{pmatrix} 1 & -1 & \sqrt{2} \\ -1 & 1 & \sqrt{2} \\ \sqrt{2} & \sqrt{2} & 0 \end{pmatrix} \quad (27.1)$$

$$S_E = \frac{1}{2} \begin{pmatrix} 1 & 1 & \sqrt{2} \\ 1 & 1 & -\sqrt{2} \\ \sqrt{2} & -\sqrt{2} & 0 \end{pmatrix} \quad (27.2)$$

Now we consider the ideal circulator and isolator. A signal entering the ideal circulator at a port n ($n = 1, 2, 3$) is transmitted to the next port in the sense of the arrow and leaves the circulator as a wave b_{n+1} . The S-matrix of the circulator is given (with port numbering according to Fig. 7) as

$$S_c = \begin{pmatrix} 0 & 0 & 1 \\ 1 & 0 & 0 \\ 0 & 1 & 0 \end{pmatrix} \quad (28)$$

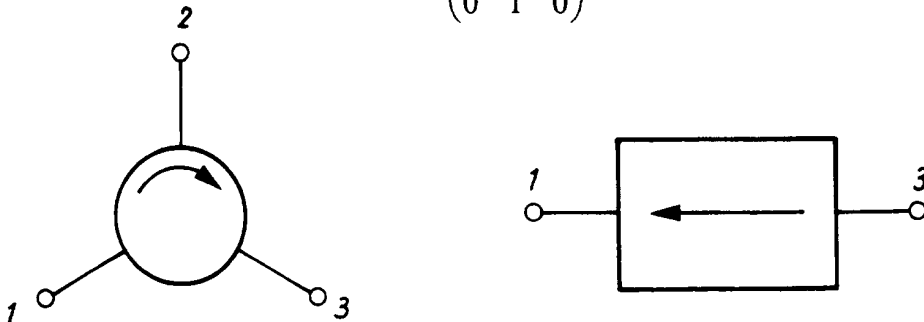


Fig. 7 3-port circulator and 2-port isolator

A circulator, like the gyrator and other passive non-reciprocal elements contains a volume of ferrite. This ferrite is normally magnetized into saturation by an external (sometimes internal) magnetic field. The magnetic properties of a saturated rf ferrite have to be characterized by a μ -tensor. The elements of this tensor are complex and strongly dependent on the bias field (resonance absorption). They represent the μ_+ and μ_- seen by a right- and left-hand circular polarized wave (with respect to the bias field) traversing the ferrite (Fig. 8). All elements of the isolator (= circulator with absorber at port 2) (Figs. 9 and 10) are zero except S_{13} , i.e. transmission from port 3 to port 1, which is 1.

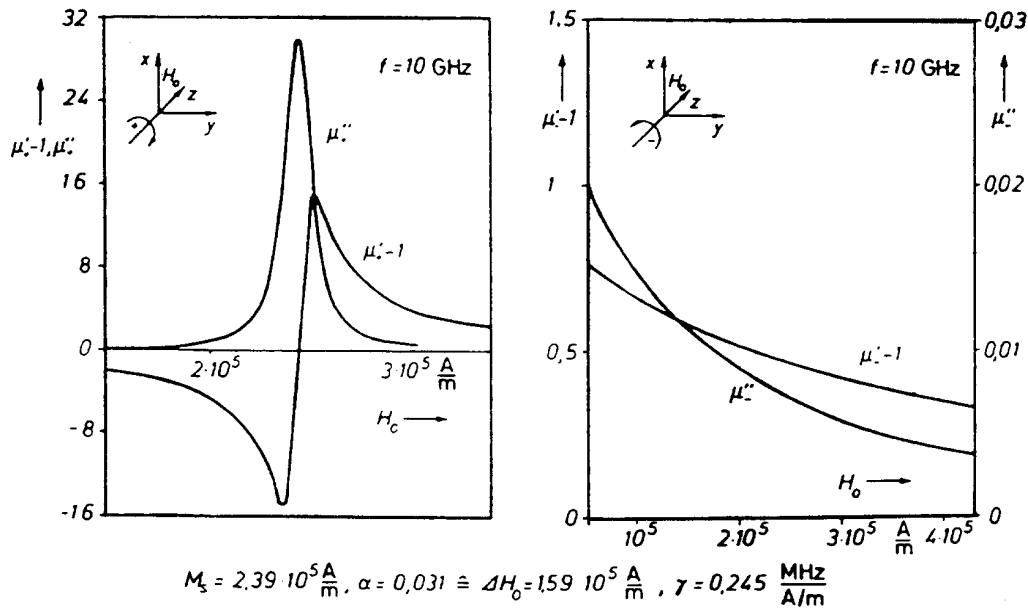


Fig. 8 Complex permeability μ_+ μ_- for circularly polarized waves in a microwave ferrite

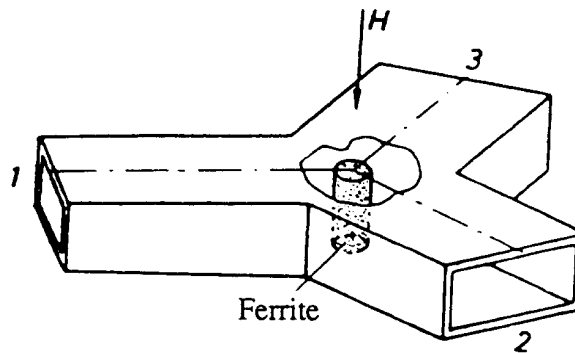


Fig. 9 Waveguide circulator

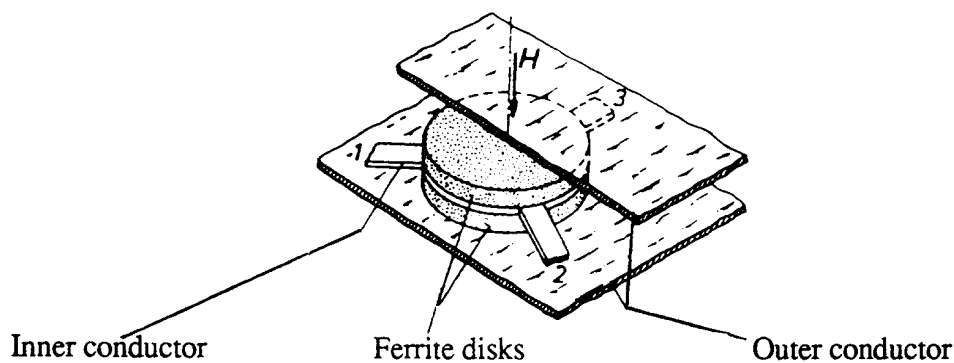


Fig. 10 Stripline circulator

It is interesting to note that all non-reciprocal elements can be made from an ideal gyrator and some other passive, reciprocal elements (often a 4-port T-hybrid or magic tee), e.g. Faraday rotation isolator, Fig. 11. Note that the frequency range of ferrite-based, non-reciprocal elements extends from about 50 MHz up to optical wavelengths (Faraday rotator) [13].

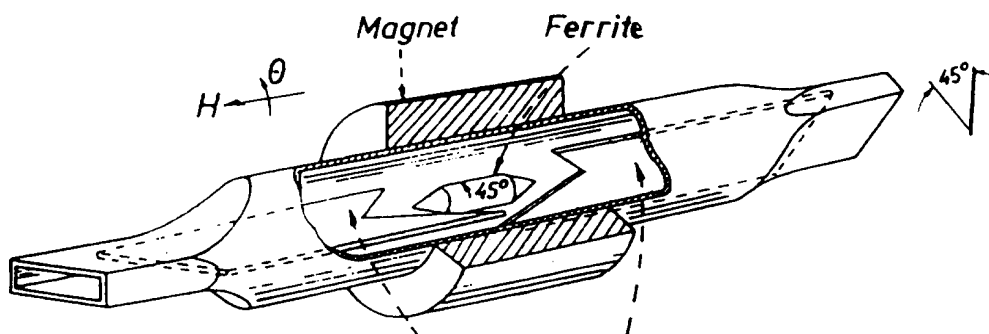


Fig. 11 Faraday rotation isolator

Exercise

Work out the S-matrix of a symmetric 6 dB resistive power splitter. Indicate the value of the inside resistor ($Z_0 = 50 \Omega$). What is the S-matrix of a symmetric lossless coaxial Y-piece?

The S-matrix of a 4-port

As a first example let us consider a combination of E-plane and H-plane waveguide "T"s (Fig. 12). This configuration is called a Magic "T" and has the S-matrix:

$$S = \frac{1}{\sqrt{2}} \begin{pmatrix} 0 & 0 & 1 & 1 \\ 0 & 0 & 1 & -1 \\ 1 & 1 & 0 & 0 \\ 1 & -1 & 0 & 0 \end{pmatrix} \quad (30)$$

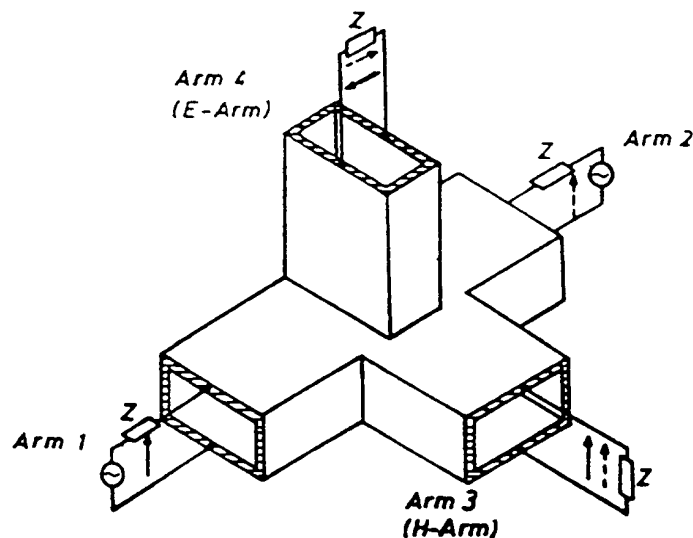


Fig. 12 Hybrid "T", Magic "T", 180° hybrid. Ideally there is no crosstalk between port 3 and port 4 nor between port 1 and port 2.

The coefficients of this S-matrix can be found by using the condition $(S^*)^T \cdot (S) = 1$ (losslessness, reciprocity and mechanical symmetry). A lossless, reciprocal 4-port may be matched at all ports and the reference plane can be chosen such that the very simple S-matrix (Eq. (30)) results. In practice, however, certain measures are required to make the E/H-"T" magic such as small stubs in the center of the tee. Today, T-hybrids are often produced not in waveguide technology, but as coaxial line and printed (planar) circuits (using also coaxial line transformers). They are widely used for signal combination or splitting in pickups and kickers for particle accelerators. In a simple vertical-loop pickup the signal outputs of the upper and lower electrodes are connected to arm 1 and arm 2, and the sum (Σ) and difference (Δ) signals are available from the H arm and E arm, respectively. This is shown in Fig. 13 assuming two generators connected to the collinear arms of the magic T. The signal from generator 1 is split (equal amplitude) into the E and H arm (for Δ and Σ ports). The signal from generator 2 propagates in the same way. We see that cancellation is produced at the Δ port (provided that both generators have equal amplitude and phase), and the sum signal shows up at the Σ port. Note that the bandwidth of a waveguide magic "T" is around one octave or the equivalent H_{10} -mode waveguide band. Broadband versions of 180° hybrids may have a frequency range from a few MHz to some GHz.

Another important element is the directional coupler. A selection of possible waveguide couplers is depicted in Fig. 13.

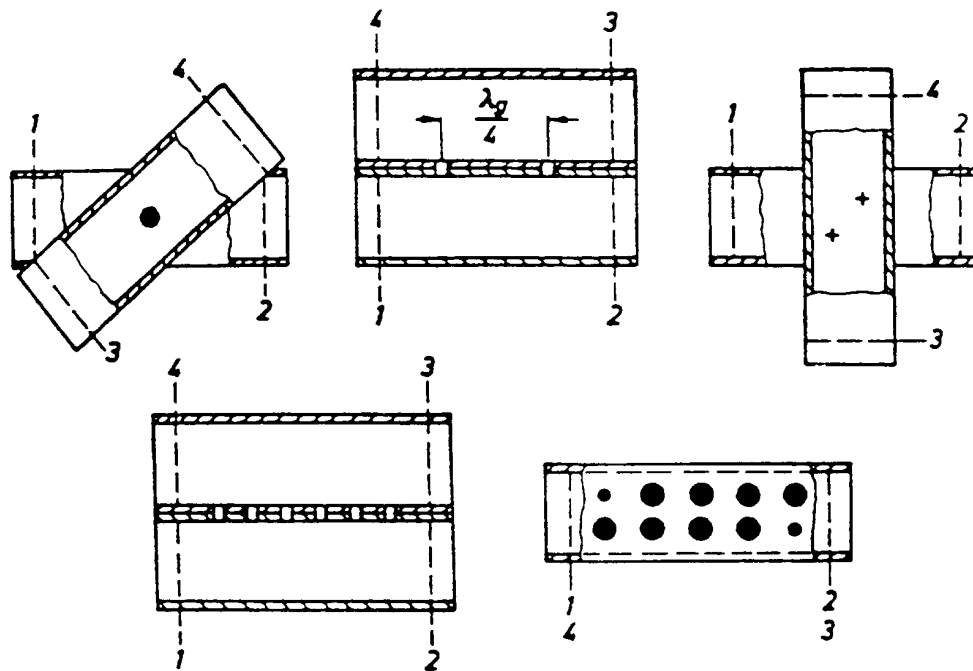


Fig. 13 Waveguide directional couplers; single-hole, double-hole and multiple-hole types.

There is a common principle of operation for all directional couplers: we have two transmission lines (waveguide, coaxial line, strip line, microstrip), and coupling is adjusted such that part of the power linked to a travelling wave in line 1 excites a (single) travelling wave in line 2. The coupler is directional when the coupled energy mainly propagates in a single travelling wave, i.e. there is no propagation in two directions.

The single-hole coupler (Fig. 13), also known as a Bethe-coupler, takes advantage of the electric and magnetic polarizability of a small ($d \ll \lambda$) coupling hole. A propagating wave in

the main line excites electric and magnetic currents in the coupling hole. Each of these currents gives rise to travelling waves in both directions. The electric coupling is independent of the angle α between the waveguides (also possible with two coaxial lines at an angle α). The magnetic coupling depends on α . For $\alpha \approx 30^\circ$ the propagating waves cancel in one direction and add in the other. The physical mechanism for the other couplers shown in Fig. 13 is similar. Each coupling hole excites waves in both directions, but the superposition of the waves coming from all coupling holes leads to a preference for a particular direction (with respect to the wave in the main line).

Example: the 2-hole, $\lambda/4$ coupler

The coupled wave leaves at port 4, the incident wave enters at port 1 (forward coupler). Optimum directivity is only obtained in a narrow frequency range where the distance of the coupling holes is roughly $\lambda/4$. For larger bandwidths, multiple hole couplers are used. The holes need not be circular; they may be slots (longitudinally or transversely orientated).

Besides waveguide couplers there exists a family of printed circuit couplers (strip line, microstrip) and also lumped element couplers (like transformers). To characterize directional couplers, two important figures are always required, i.e. *coupling* and *directivity*. For the elements shown in Fig. 13, the coupling appears in the S-matrix as the coefficient

$$|S_{13}| = |S_{31}| = |S_{42}| = |S_{24}|$$

with $\alpha_c = -20 \log |S_{13}|$ [dB] being the coupling attenuation.

The *directivity* is the ratio of the *desired* coupled wave to the *undesired* (i.e. wrong direction) coupled wave, e.g.

$$\alpha_d = 20 \log \frac{|S_{31}|}{|S_{41}|} \quad \text{directivity [dB]}.$$

Practical numbers for the coupling are 3 dB, 6 dB, 10 dB, and 20 dB with directivities usually better than 20 dB. Note that the ideal 3-dB coupler (like most directional couplers) often has a $\pi/2$ phase shift between the main line and the coupled line (90° hybrid). The following relations hold for an ideal directional coupler with properly chosen reference planes

$$\begin{aligned} S_{11} &= S_{22} = S_{33} = S_{44} = 0 \\ S_{21} &= S_{12} = S_{43} = S_{34} \\ S_{31} &= S_{13} = S_{42} = S_{24} \\ S_{41} &= S_{14} = S_{32} = S_{23} \end{aligned} \tag{31.1}$$

$$S = \begin{pmatrix} 0 & \sqrt{1-|S_{13}|^2} & \pm j|S_{13}| & 0 \\ \sqrt{1-|S_{13}|^2} & 0 & 0 & \pm j|S_{13}| \\ \pm j|S_{13}| & 0 & 0 & \sqrt{1-|S_{13}|^2} \\ 0 & \pm j|S_{13}| & \sqrt{1-|S_{13}|^2} & 0 \end{pmatrix} \tag{31.2}$$

and for the 3 dB coupler ($\pi/2$ -hybrid)

$$S_{3dB} = \frac{1}{\sqrt{2}} \begin{pmatrix} 0 & 1 & \pm j & 0 \\ 1 & 0 & 0 & \pm j \\ \pm j & 0 & 0 & 1 \\ 0 & \pm j & 1 & 0 \end{pmatrix}. \quad (31.3)$$

As further examples of 4-ports, the 4-port circulator and the one-to-three power divider should be mentioned. In general, one must keep in mind that a port is assigned to each waveguide or TEM-mode considered. Since for waveguides the number of propagating modes increases with frequency, a 2-port will become a $2n$ -port at lower frequencies (Fig. 14). Also a TEM line beyond cutoff is a multiport. In certain cases modes below cutoff may be taken into account, e.g. for calculation of the scattering properties of waveguide discontinuities, using the S-matrix approach.

There are different technologies for realizing microwave elements such as directional couplers and T-hybrids. Examples are the stripline coupler shown in Fig. 15, the 90° , 3-dB coupler Fig. 16 and the printed circuit magic T Fig. 17.

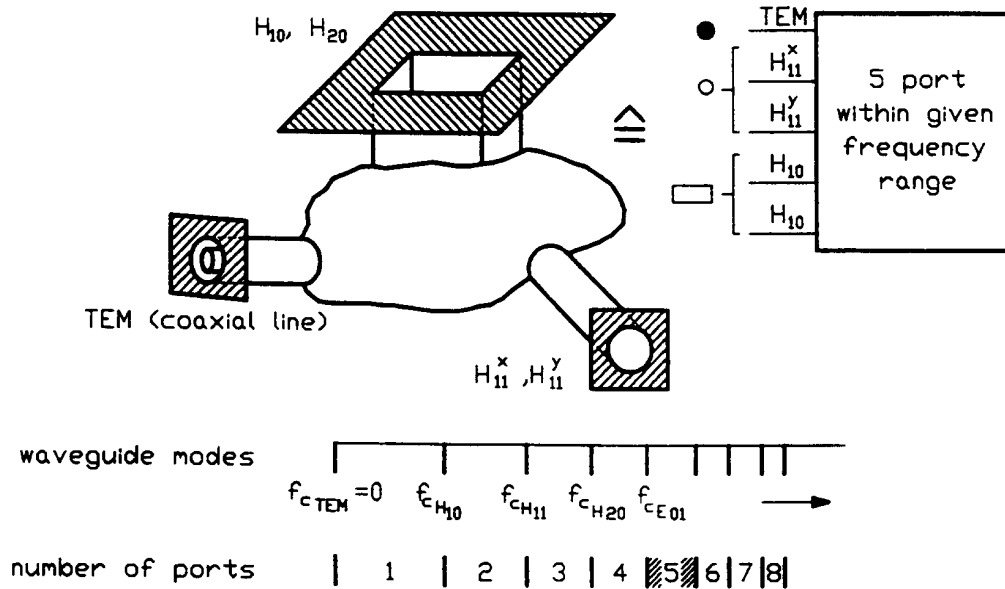


Fig. 14 Example of a multiport

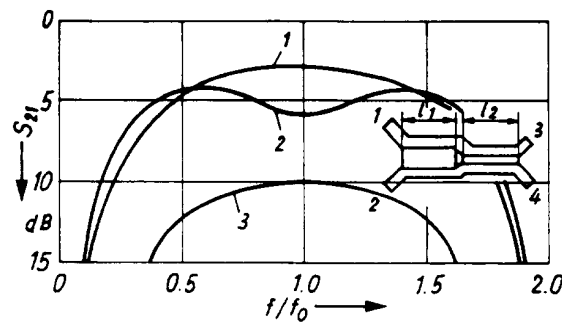


Fig. 15 Stripline directional coupler (2-stage); curve 1) 3-dB coupler, 3) 10-dB coupler, 2) broadband 5-dB coupler (cascaded 3-dB and 10-dB coupler) [2].

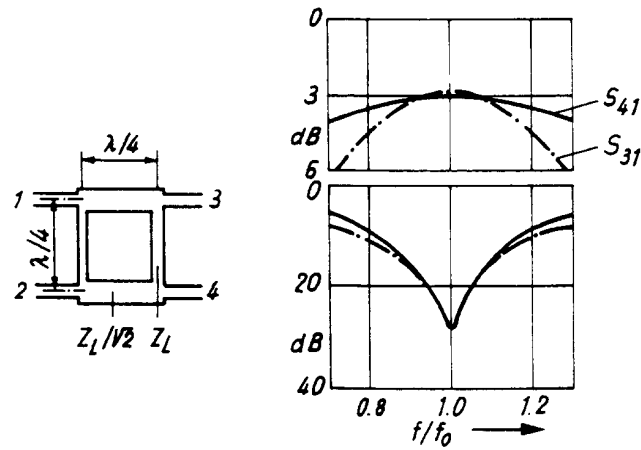


Fig. 16 90°, 3-dB coupler [2]

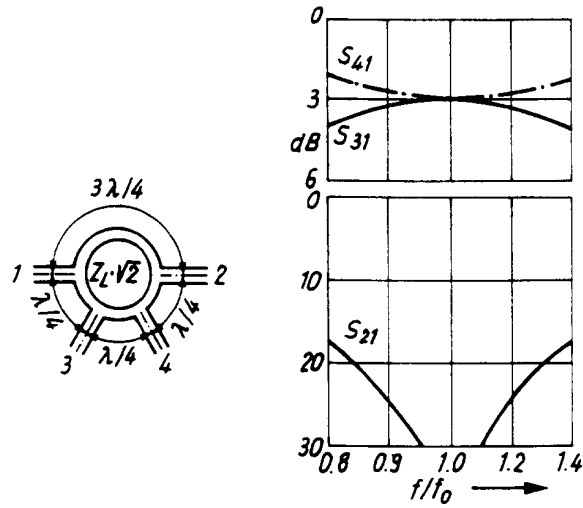


Fig. 17 Magic T in a printed circuit version [2]

5. BASIC PROPERTIES OF STRIPLINES, MICROSTRIP AND SLOTLINES

5.1 Striplines

A stripline is a flat conductor between a top and bottom ground plane. The space around this conductor is filled with a homogeneous dielectric material. This line propagates a TEM mode. With the static capacity per unit length, C' , and the permittivity of the dielectric, ϵ_r , the characteristic impedance Z_0 of the line is given by

$$Z_0 = \sqrt{\frac{L'}{C'}}$$

$$v_{ph} = \frac{c}{\sqrt{\epsilon_r}} = \frac{1}{\sqrt{L'C'}}$$

$$Z_0 = \sqrt{\epsilon_r} \cdot \frac{1}{C'_c} \quad (34)$$

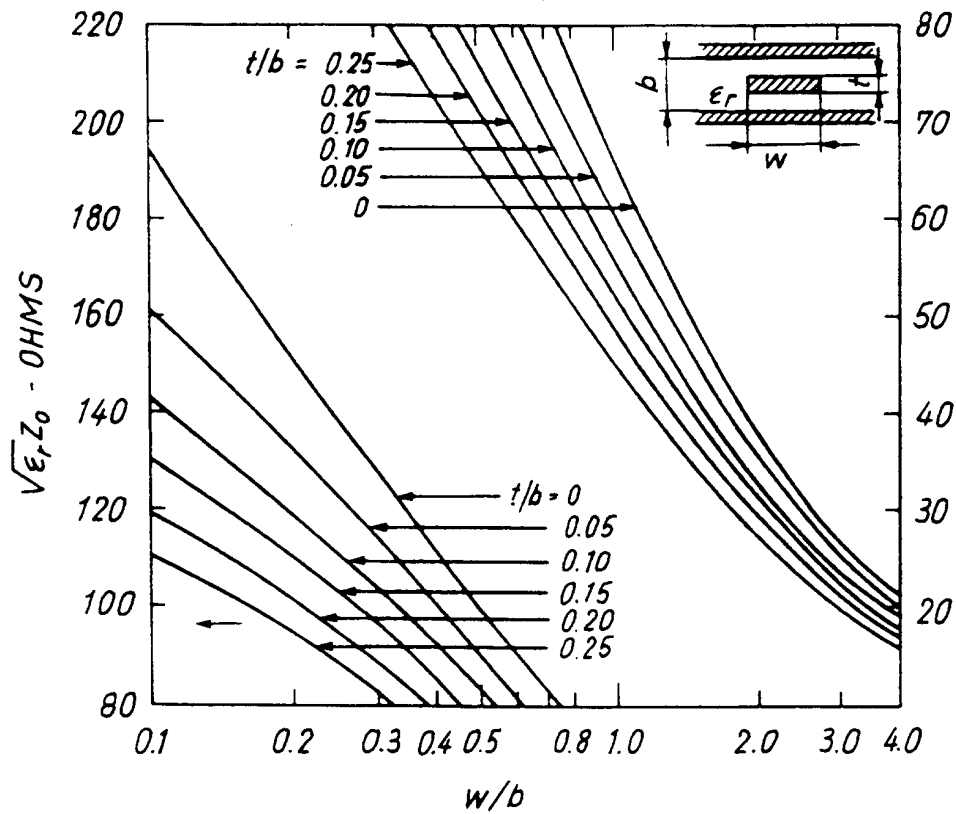


Fig. 18 Characteristic impedance of striplines [14]

For a mathematical treatment, the effect of the fringing fields may be described in terms of static capacities (see Fig. 19) [14]. The total capacity then becomes

$$C_{tot} = C_{p1} + C_{p2} + C_{f1} + 2C_{f2}. \quad (35)$$

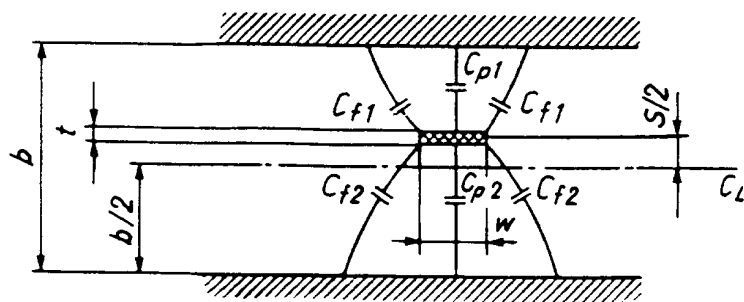


Fig. 19 Design, dimensions, and characteristics for offset center-conductor strip transmission line [14]

For striplines with an homogeneous dielectric the phase velocity is the same, and frequency independent, for all TEM-modes. A configuration of two coupled striplines (3-conductor system) may have two independent TEM-modes (odd mode, even mode, cf. Fig. 20).

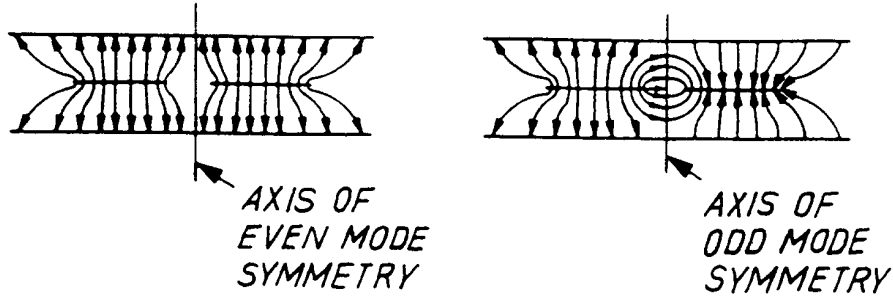


Fig. 20 Even and odd mode in coupled striplines [14]

The analysis of coupled striplines is required for the design of directional couplers. Besides the phase velocity the odd and even mode impedances Z_{0o} and Z_{0e} must be known.

$$Z_{0e} = \frac{94.15\Omega/\sqrt{\epsilon}}{w/b + \ln 2/\pi + (1/\pi) \cdot \ln\left(\left\{1 + \tanh\left[(\pi/2)(s/b)\right]\right\}\right)} \quad (36)$$

$$Z_{0o} = \frac{94.15\Omega/\sqrt{\epsilon}}{w/b + \ln 2/\pi + (1/\pi) \cdot \ln\left(\left\{1 + \coth\left[(\pi/2)(s/b)\right]\right\}\right)} \quad (37)$$

Equations (36) and (37) are also known as Cohn nomographs in a graphical presentation and are valid as a good approximation for the structure shown in Fig. 21. For a quarter-wave directional coupler (single section in Fig. 21a) very simple design formulae can be given

$$Z_{0o} = \sqrt{\frac{1+C_0}{1-C_0}}$$

$$Z_{0e} = \sqrt{\frac{1-C_0}{1+C_0}}$$

$$Z_0 = \sqrt{Z_{0o}Z_{0e}}$$

$$\text{Coupling [dB]} = 20 \log C_0. \quad (38)$$

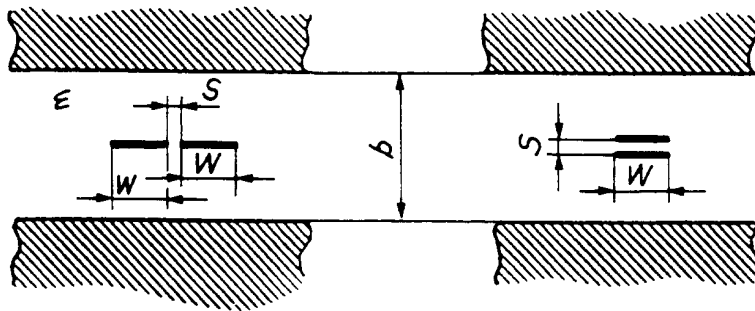


Fig. 21 Types of coupled striplines [14], strip width = W, spacing = S

Note that couplers of this type are backward couplers (in contrast to the 2-hole waveguide coupler), i.e. the coupled wave leaves the coupler in the opposite direction to the in-coming wave.

The stripline coupler technology is rather widespread by now, and very cheap high quality elements are available in a wide frequency range. An even simpler way to make such devices is to use a section of shielded 2-wire cable. Later in this course [15], we will hear in more detail about such couplers as they play an important role in beam diagnostics and for stochastic cooling.

5.2 Microstrip

A microstripline may be visualized as a stripline with the top cover and top dielectric layer taken away (Fig. 22). It is thus an asymmetric open structure, and only part of its cross section is filled with a dielectric material. Since there is a transversely inhomogeneous dielectric, only a quasi-TEM wave exists. This has several implications such as a frequency-dependent characteristic impedance and a considerable dispersion (Fig. 23).

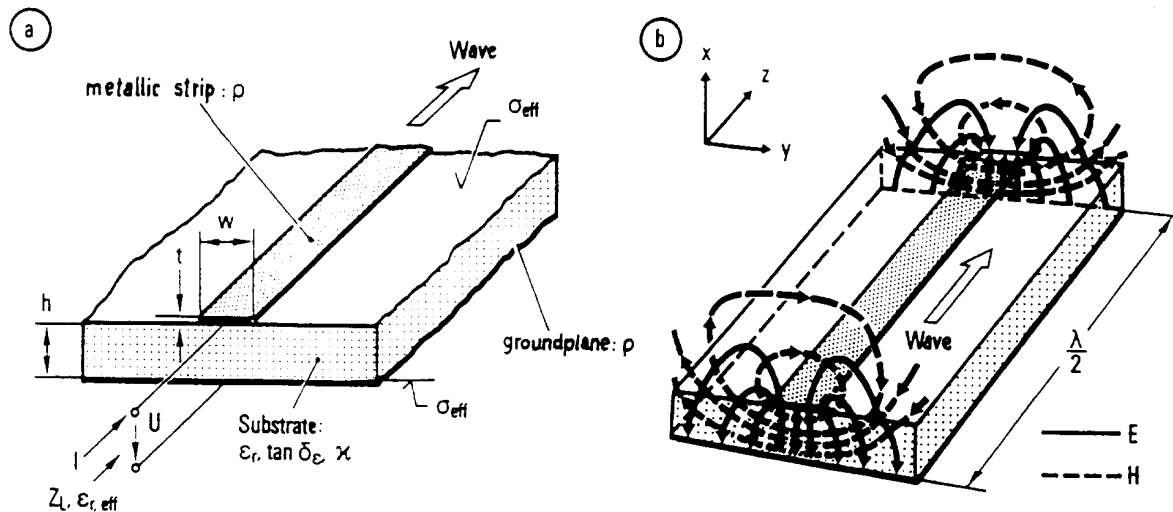


Fig. 22 Microstripline a) Mechanical construction, b) Static field approximation [16].

An exact field analysis for this line is rather complicated and there exists a considerable number of books and other publications on the subject [16, 17]. Due to the dispersion of the microstrip, the calculation of coupled lines and thus the design of couplers and related structures is also more complicated than in the case of the stripline. Microstrips tend to **radiate** at all kind of discontinuities such as bends, changes in width, through holes etc.

With all the disadvantages mentioned above in mind, one may question why they are used at all. The main reasons are the cheap production, once a conductor pattern has been defined, and easy access to the surface (integration of active elements). Microstrip circuits are also known as MIC's = Microwave Integrated Circuits. A further technological step is the MMIC (Monolithic Microwave Integrated Circuit) where active and passive elements are integrated on the same semiconductor substrate.

In Figs. 24 and 25 various planar printed transmission lines are depicted. The microstrip with overlay is relevant for MMICs and the strip dielectric wave guide is a "Printed Optical Fibre" for millimeter-waves and integrated optics [17].

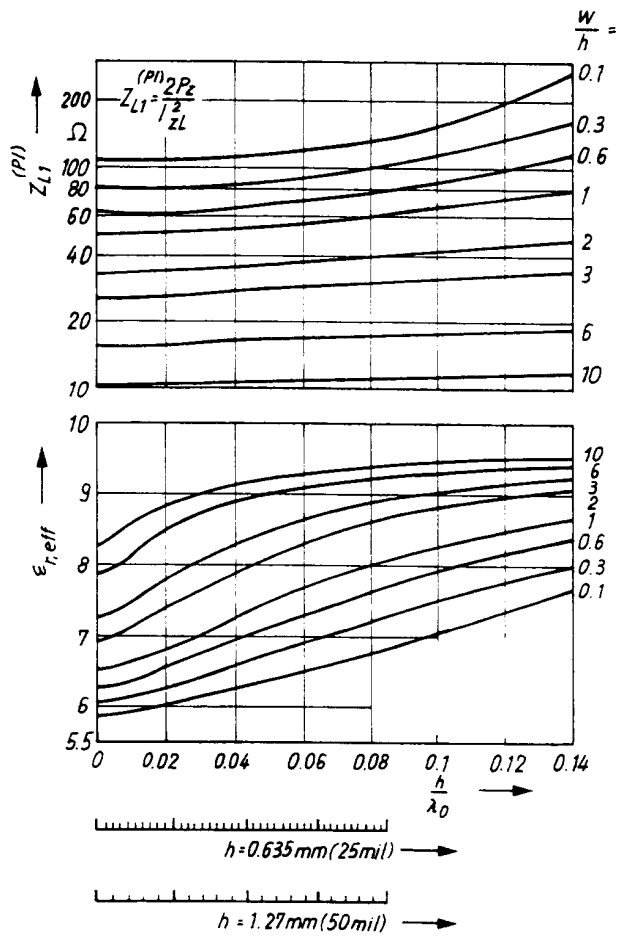


Fig. 23 Characteristic impedance (current/power definition) and effective permittivity of microstripline [16]

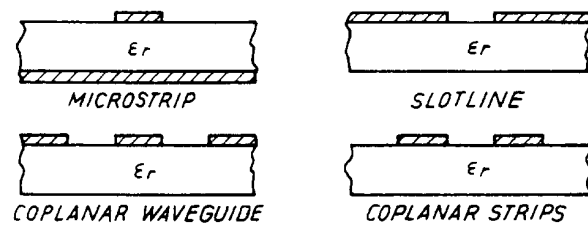


Fig. 24 Planar transmission lines used in MIC

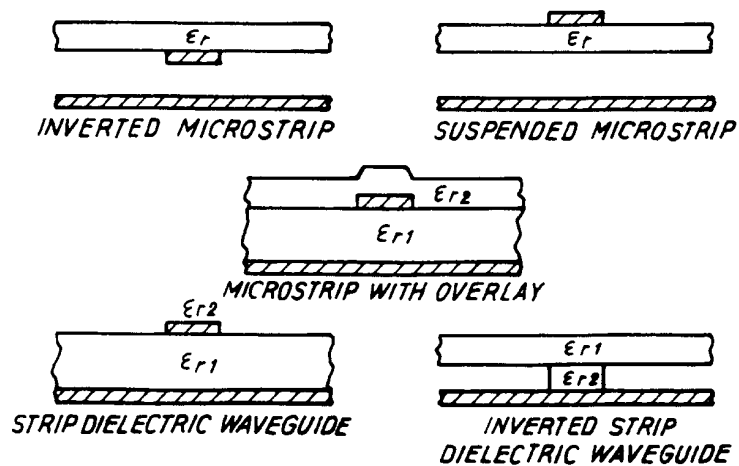


Fig. 25 Various transmission lines derived from microstrip [17]

5.3 Slotlines

The slotline may be considered to be a dual structure to the microstrip. It is essentially a slot in the ground plane metallisation of a metallized dielectric substrate as shown in Fig. 26. The characteristic impedance and the effective dielectric constant exhibit similar dispersion properties to those of the microstripline. A unique feature of the slotline is that it may be combined with microstriplines on the same substrate. This, in conjunction with through holes, permits interesting topologies such as pulse inverters in sampling heads (e.g. for sampling scopes).

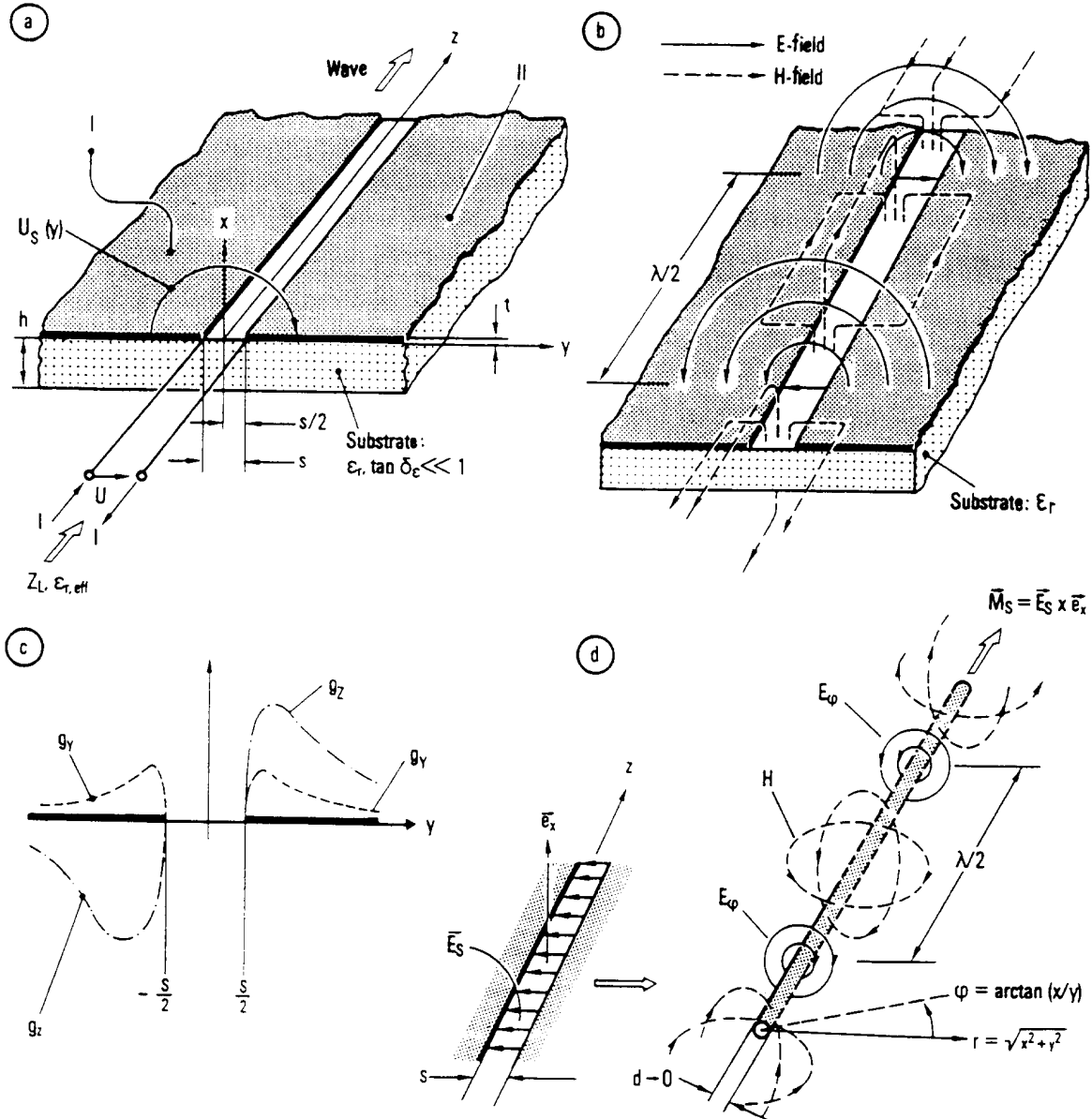


Fig. 26 Slotlines a) Mechanical construction, b) Field pattern (TE approximation), c) Longitudinal and transverse current densities, d) Magnetic line current model [16]

Figure 27 shows a broadband (decade bandwidth) pulse inverter. Assuming the upper microstrip to be the input, the signal leaving the circuit on the lower microstrip is inverted since this microstrip ends on the opposite side of the slotline compared to the input. Printed slotlines are also used for broadband pickups in the GHz range (e.g. Stochastic Cooling) [15].

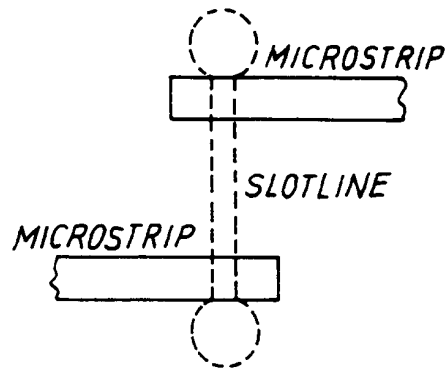


Fig. 27 Two microstrip-slotline transitions connected back to back for 180° phase [17]

6. APPLICATION OF THE SMITH CHART

A useful and very common tool for both measurements and calculations on rf components is the Smith Chart (S.C.) shown in Fig. 28. It indicates in the plane of the complex reflection coefficient ρ the corresponding values of the complex terminating impedance $Z = R + jX$ (Fig. 28a).

$$\rho = \frac{Z - Z_0}{Z + Z_0} \quad (39)$$

or in terms of the admittance $Y = G + jB$ (Fig. 28b)

$$\rho = -\frac{Y - Y_0}{Y + Y_0} \quad (40)$$

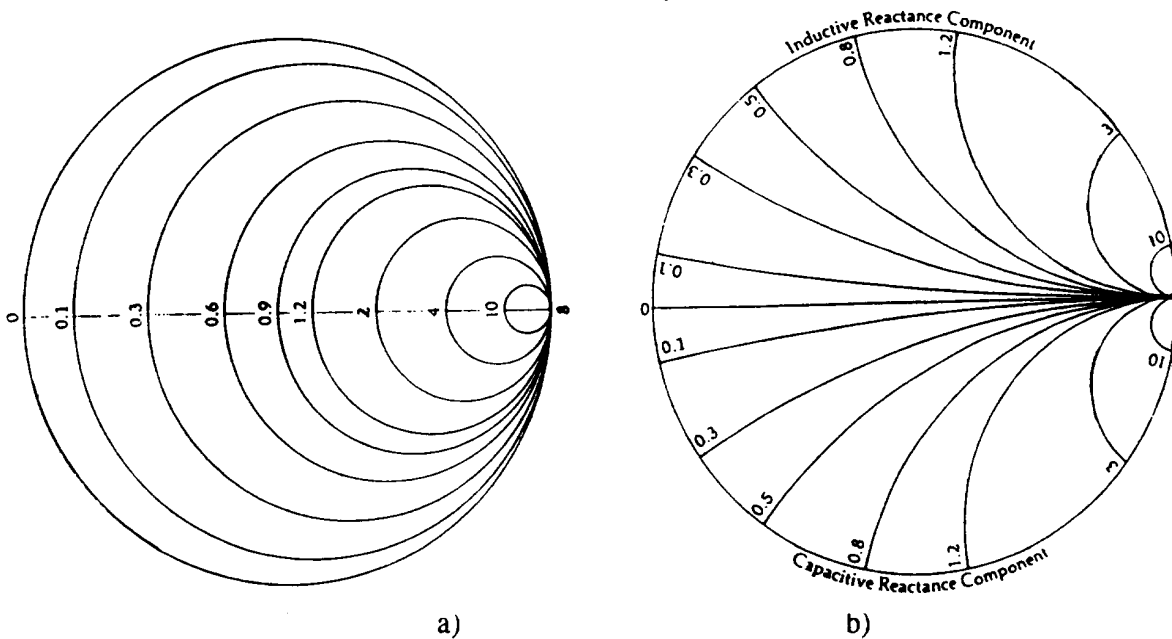


Fig. 28 Construction of the Smith Chart a) Constant resistance circles b) Constant reactance circles

Generalized circles (straight line = circle with $R \Rightarrow \infty$ convert into generalized circles, when going from the Z-plane to the ρ -plane). In practice one transforms a circle from the Z-plane with three points (but not the center) into a circle in the ρ -plane. Note that indicating a coordinate in the Smith Chart without specifying Z_0 or Y_0 is meaningless since the S.C. is mostly normalized to Z_0 . Changing the normalization from Z_0 to Y_0 (required when adding admittances) does not change ρ , but the system of circle coordinates is turned by 180° .

Combining Figs. 28a and 28b produces the Smith Chart in the ρ -plane (Fig. 29).

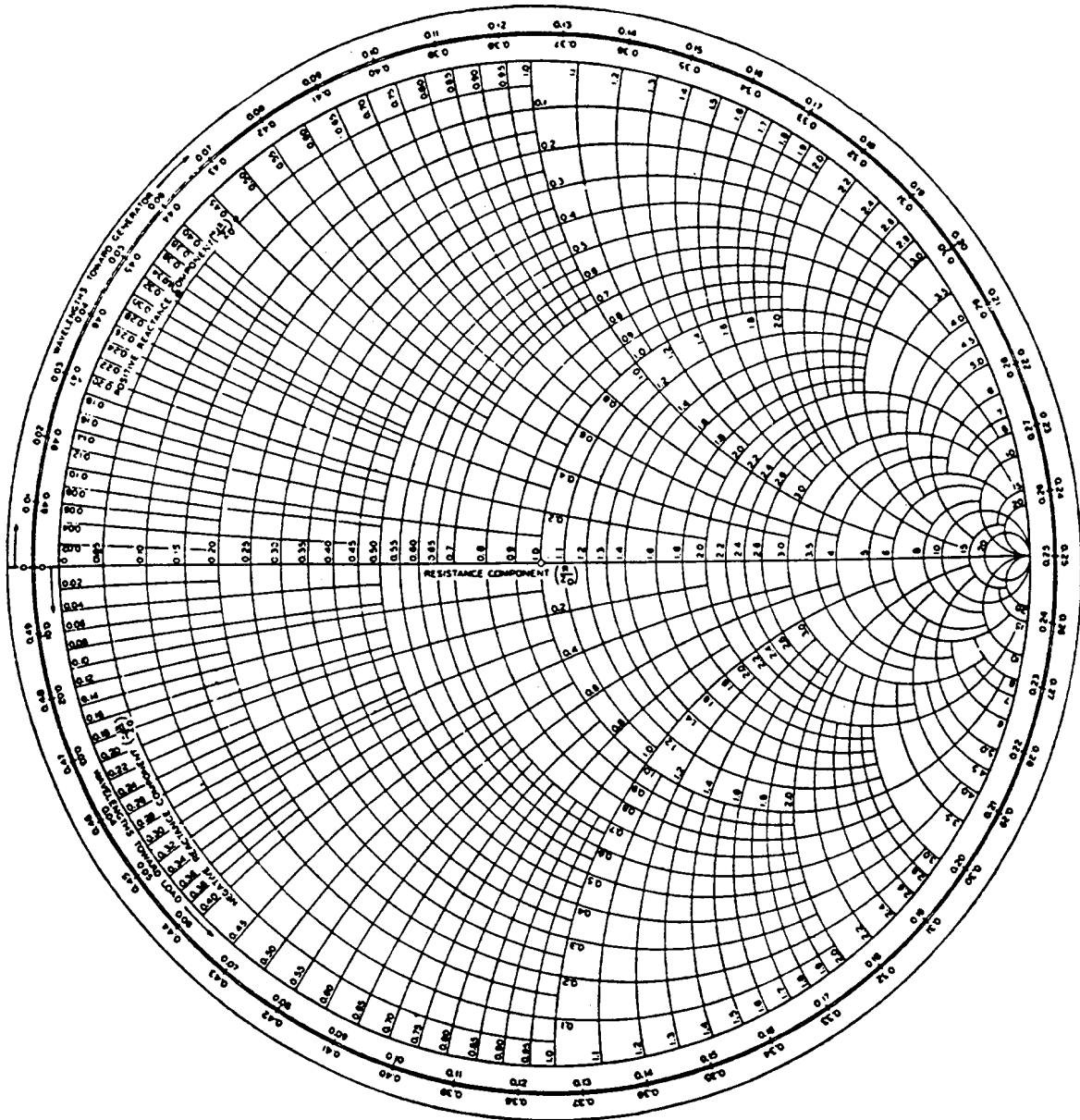


Fig. 29 Smith Chart

All real and imaginary values on the Smith Chart are normalized to a characteristic impedance or admittance Z_0 or Y_0 e.g.

$$z = r + jx = \frac{R}{Z_0} + j\frac{X}{Z_0} \text{ and } y = g + jb = \frac{G}{Y_0} + j\frac{B}{Y_0}$$

Exercise: Imagine a Cartesian coordinate system superimposed and visualize a few important reference points.

$\rho = 0$	$R/Z_0 = 1$	$X/Z_0 = 0$	Matched load
$\rho = -1$	$R/Z_0 = 0$	$X/Z_0 = 0$	Short
$\rho = +1$	$R/Z_0 = \infty$	$X/Z_0 = \infty$	Open
$\rho = +j$	$R/Z_0 = 0$	$X/Z_0 = +1$	Shorted $\lambda/8$ line (Z_0)
$\rho = -j$	$R/Z_0 = 0$	$X/Z_0 = 1$	Shorted $3\lambda/8$ line (Z_0)

The loci of constant real and imaginary part are obtained from Eqs. (39) and (40) (conformal mapping).

As a further exercise one may read modules and phase of ρ for a few impedances:

$Z_1 = 25 \Omega$	$Z_0 = 50 \Omega$	
$Z_2 = 100 \Omega$	$Z_0 = 50 \Omega$	
$Z_3 = 50 + j50 \Omega$	$Z_0 = 50 \Omega$	Try also parallel and serial
$Z_4 = 50 + j50 \Omega$	$Z_0 = 100 \Omega$	combinations of $Z_1 \dots Z_6$
$Z_5 = +j 200 \Omega$	$Z_0 = 50 \Omega$	
$Z_6 = 100 - j 25 \Omega$	$Z_0 = 100 \Omega$	

Impedances are added in an S. C. normalized to Z_0 when they are connected in series. Admittances are added in an S. C. normalized to Y_0 (parallel connections).

Adding a lossless line to a given impedance (length of the line = ℓ/λ means turning ρ clockwise by $4\pi \times \ell/\lambda$ i.e. $\pi/2$ for $\lambda/8$, π for $\lambda/4$, etc. The modulus of π does not change after a transformation over a lossless line which if it is of the $\lambda/4$ type is often used as a transformer ($\lambda/4$ transformer) and with Z_1 = termination impedance of the line and Z_2 = input impedance we obtain

$$Z_1 Z_2 = Z_0^2 \quad (\lambda / 4 \text{ transformer}). \quad (41)$$

However, for practical applications the bandwidth of a single $\lambda/4$ transformer is often not sufficient. Thus multistage line transformers are used which, treated in the Smith Chart means renormalization for each line impedance.

Transformation over a lossy line leads to a logarithmic spiral which is not easy to draw (pointwise construction). Consider a lossy parallel resonance circuit (R, L, C) in the complex Z-plane. The locus of impedance is a circle symmetric to the positive real axis, intersecting at $Z = 0$ ($f = 0, \infty$) and $Z = R$ ($f = f_0$). This circle can be transformed easily into the ρ -plane (conformal mapping). Use symmetry to the real axis and $Z = R$ into $\rho = -1$ and $\rho = (R-Z_0)/(R+Z_0)$. In practice the transformation of the point $Z = 0$ is unrealistic because $f = 0$ or ∞ . Thus one should use some other convenient frequency.

The dashed line in Fig. 30 can be seen directly on a vector network analyzer equipped with a polar display. Numbers of interest are

$$\left. \begin{array}{l} \text{Unloaded } Q = Q_0 \\ \text{External } Q = Q_{ex} \\ \text{Loaded } Q = Q_L \end{array} \right\} f_0 = \text{res. frequency}$$

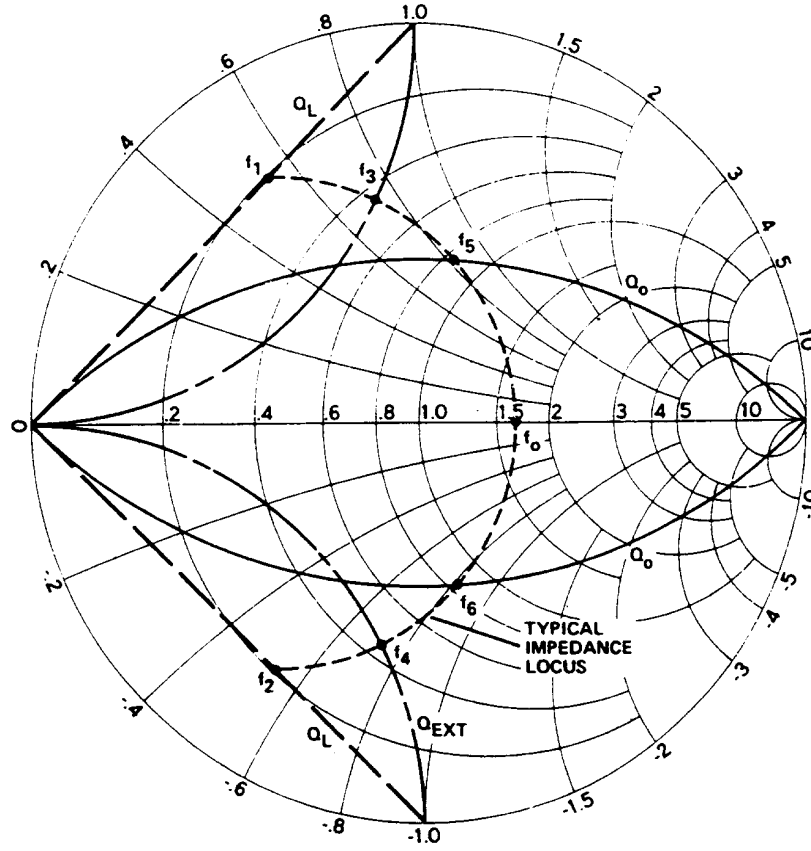


Fig. 30 Loci of Q_0 , Q_L and Q_{EXT} of a resonator

$$\frac{1}{Q_L} = \frac{1}{Q_0} + \frac{1}{Q_{ext}} \quad (42)$$

$$Q = \frac{f_0}{\Delta f} \quad (3 \text{ dB}).$$

Referring to Fig. 30 we obtain

$$\begin{aligned} Q_0 &= f_0 / (f_5 - f_6) \\ Q_L &= f_0 / (f_1 - f_2) \\ Q_{ext} &= f_0 / (f_3 - f_4) \end{aligned} \quad (43)$$

Figure 30 shows the resonator in the "detuned short position", i.e. the impedance of the resonator far from f_0 approaches zero and f_1, f_2 are "half-power" points (intersection with straight lines connecting $\rho = 0$ and $\rho = \pm j$ respectively). For the external Q (f_3, f_4) we must turn the locus of the resonator into "detuned open position" ($\lambda/4$ transformer). This produces an intersection with the constant reactance circle $Z = Y/Z_0 = \pm j$. Finally the points f_5, f_6 (Q_0 ; $R_{cavity} = \pm X_{cavity}$) are read from the intersection of a cavity with two circles centered at $\pm j$ and having a radius of $\sqrt{2}$.

There are three ranges of the coupling factor β defined by

$$\beta = \frac{Q_0}{Q_{ext}}$$

and

$$Q_L = \frac{Q_0}{1 + \beta} \quad (44)$$

This then allows us to define:

- **Critical Coupling:** $\beta = 1$, $Q_L = Q_0/2$. The locus of ρ touches the center of the S.C.
- **Undercritical Coupling:** ($0 < \beta < 1$). Locus of ρ in the detuned short position is left of the center of the S.C.
- **Overcritical coupling:** ($1 < \beta < \infty$). The center of the S.C. is inside the locus of ρ .

Caution: when using a network analyzer with a Cartesian display for $|\rho|$ one cannot decide from $|\rho|$ only whether one has over or undercritical coupling; the phase of the complex reflection factor ρ is required for this.

- Undercritical coupling \Rightarrow phase swing $< 180^\circ$
- Critical coupling \Rightarrow phase swing $= 180^\circ$
- Overcritical coupling \Rightarrow phase swing $> 180^\circ$.

ACKNOWLEDGEMENTS

The author would like to thank A. Fiebig, R.K. Hoffmann, E. Jensen and C. Taylor for stimulating discussions and for reading the manuscript.

REFERENCES

- [1] K. Kurokawa, Power waves and the scattering matrix, IEEE-T-MTT, Vol. 13 No 2, March 1965, 194-202.
- [2] H. Meinke, F. Gundlach, Taschenbuch der Hochfrequenztechnik, 4. Auflage, Springer, Heidelberg, 1986, ISBN 3-540-15393-4.
- [3] K.C. Gupta, R. Garg, and R. Chadha, Computer-aided design of microwave circuits, Artech, Dedham, MA 1981, ISBN 0-89006-106-8.
- [4] B. Schiek, Meßsysteme der Hochfrequenztechnik, ELTEX, Hüthig, Heidelberg, 1984, ISBN 3-7785-1045.
- [5] C. Bowick, rf circuit design, H.W. Sams and Co., Indianapolis 1989, ISBN 0-672-21868-2.
- [6] R.W. Anderson, S-parameter techniques for faster, more accurate network design, Hewlett-Packard Application Note 95-1.

- [7] S-parameter design, Hewlett-Packard Application Note 154.
- [8] P.C.T. Yip, High-frequency circuit design and measurements, Chapman and Hall, London 1980.
- [9] W.S. Cheung, F.H. Lertien, Microwaves made simple, Principles and applications, Artech, Dedham, MA 1985, ISBN 0-89006-173-4.
- [10] Microwave network analyzer applications, Hewlett-Packard Application Note AN 117.
- [11] S.J. Mason, Feedback theory - Some properties of signal flow graphs, Proc. IRE, Vol. 41, Sept. 1953, 1144-1156.
- [12] A. Fiebig, Lineare Signalflußdiagramme, Archiv der Elektrischen Übertragung (AEÜ) 15(1961), 285-292.
- [13] H. Entschladen, Passive nichtreziproke Bauelemente der Mikrowellentechnik, Elektronik Anzeiger No. 11, 1971, 217-223.
- [14] H. Howe, Stripline circuit design, Artech, Dedham, MA 1982, 4th Edition, ISBN 0-89006-020-7.
- [15] C. Taylor, Microwave kickers and pickups, this course.
- [16] R.K. Hoffmann, Integrierte Mikrowellenschaltung, Springer, Heidelberg, 1983, ISBN 3-540-12352-0, (also available in English version).
- [17] K.C. Gupta, R. Garg, and I. Bahl, Microstrip lines and slotlines, Artech Dedham, MA 1979, ISBN 0-89006-074-6.

